OPEN ACCESS

REPORT

The Innovation Geoscience

Mechanisms utilized by *Methanobacterium* sp. YSL for growth on zero-valent iron

Shiling Zheng,[1] Xin Li,[1] Fanghua Liu,[1,2,3,4,*] Derek R. Lovley,[5] and Dawn E. Holmes[5,6]

*Correspondence: fhliu@yic.ac.cn

Received: January 8, 2025; Accepted: September 11, 2025; Published Online: September 15, 2025; https://doi.org/10.59717/j.xinn-geo.2025.100166

GRAPHICAL ABSTRACT

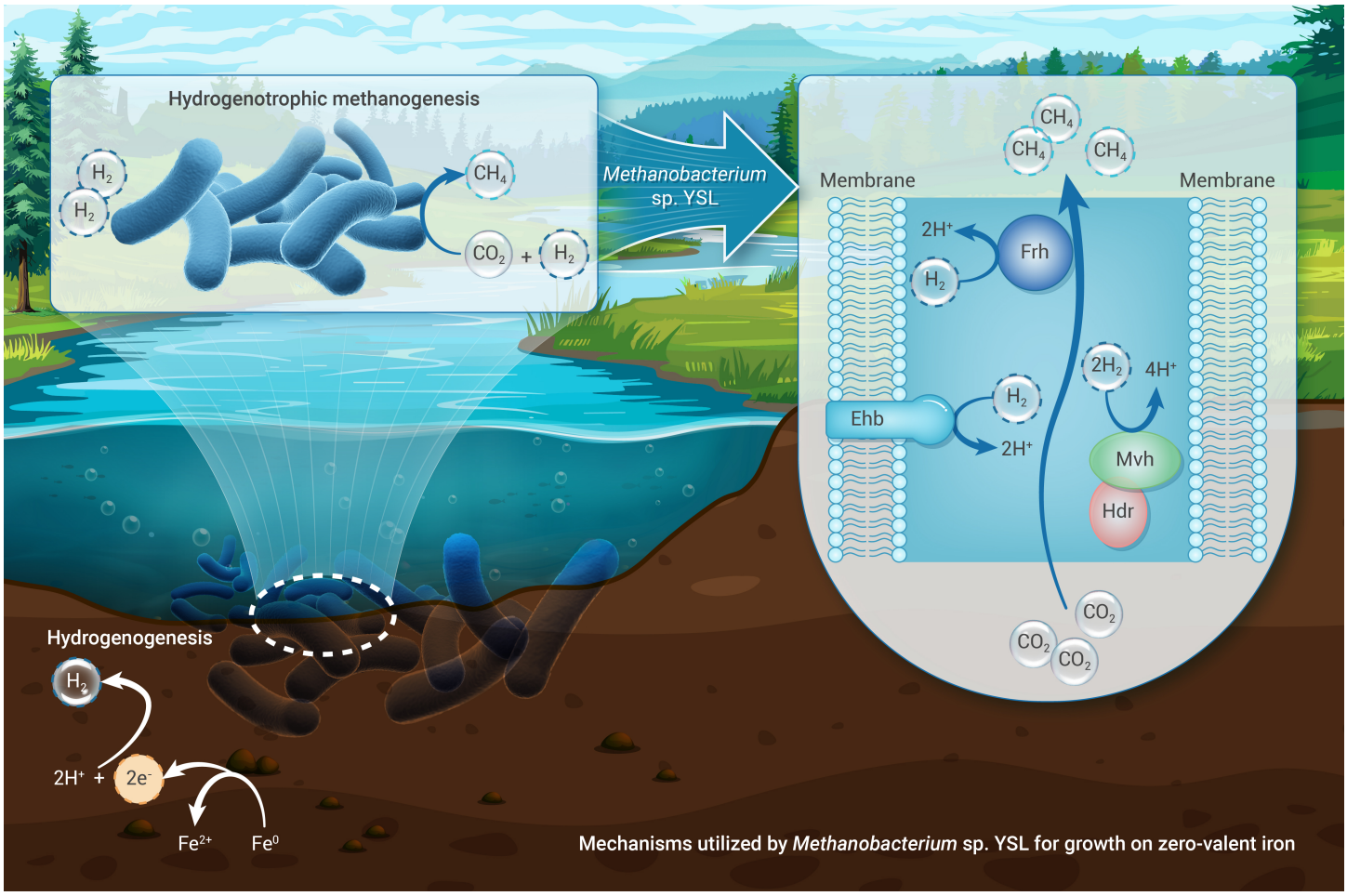

PUBLIC SUMMARY

- Strain YSL employs H_2 as an intermediary electron carrier to extract electrons from zero-valent iron.
- Mutations in key subunits of the Eha complex likely render it nonfunctional in strain YSL.
- Cytoplasmic hydrogenases compensate for Eha's inactivity and enable slow H_2-dependent growth of strain YSL.
- The results emphasize the environmental importance of microbial reactions that seem slow in lab culture.

REPORT

www.the-innovation.org/geoscience

Mechanisms utilized by *Methanobacterium* sp. YSL for growth on zero-valent iron

Shiling Zheng,[1] Xin Li,[1] Fanghua Liu,[1,2,3,4,*] Derek R. Lovley,[5] and Dawn E. Holmes[5,6]

[1]Shandong Key Laboratory of Coastal Environmental Processes, Yantai Institute of Coastal Zone Research, Chinese Academy of Sciences, Yantai 264003, China

[2]Laboratory for Marine Biology and Biotechnology, Qingdao Marine Science and Technology Center, Qingdao 266237, China

[3]Guangdong Key Laboratory of Integrated Agro-environmental Pollution Control and Management, Institute of Eco-environmental and Soil Sciences, Guangdong Academy of Sciences, Guangzhou 510650, China

[4]National-Regional Joint Engineering Research Center for Soil Pollution Control and Remediation in South China, Guangzhou 510650, China

[5]Department of Microbiology, University of Massachusetts, Amherst, Massachusetts 01003, USA

[6]Department of Physical and Biological Science, Western New England University, Springfield, Massachusetts 01119, USA

*Correspondence: fhliu@yic.ac.cn

Received: January 8, 2025; Accepted: September 11, 2025; Published Online: September 15, 2025; https://doi.org/10.59717/j.xinn-geo.2025.100166

Citation: Zheng S., Li X., Liu F., et al. (2025). Mechanisms utilized by *Methanobacterium* sp. YSL for growth on zero-valent iron. *The Innovation Geoscience* **3**:100166.

Electrobiocorrosion (i.e. direct metal-to-microbe electron transfer) is a recently recognized, highly aggressive form of microbial metal corrosion. *Methanobacterium subterraneum* strain YSL grows as an electron accepting partner in direct interspecies electron transfer, suggesting that it might have the capacity for electrobiocorrosion. To evaluate this possibility, strain YSL was grown with either pure Fe^0, which abiotically generates H_2, or 316L stainless steel, which does not generate H_2, as the sole potential electron donor. There was a steady accumulation of H_2 in uninoculated controls with Fe^0. No H_2 was detected in strain YSL cultures with Fe^0. Rather, strain YSL produced methane at a rate consistent with conversion of the H_2 abiotically generated from Fe^0 to methane. Strain YSL did not produce methane in incubations with stainless steel. These results indicated that strain YSL relies on H_2 as an intermediary electron carrier between Fe^0 and cells, a result in conflict with the previous report that strain YSL was incapable of H_2 utilization. Further investigation revealed that strain YSL can grow on H_2, but more than 50-fold slower than is typical for other *Methanobacterium* strains. Genomic analysis revealed that mutations in genes for seven subunits of Eha, the primary energy-converting hydrogenase of *Methanobacterium* species, likely disabled its function in strain YSL. Proteomic analysis suggested that a compensatory high expression of cytoplasmic hydrogenases enabled slow growth on H_2. These studies highlight the importance of analyzing slow metabolic capabilities, which are difficult to detect with standard methods yet can have significant environmental consequences.

INTRODUCTION

The mechanisms for microbial corrosion of ferrous metals are of interest because of its substantial economic burden.[1-3] Methanogenic microorganisms are often associated with corroding iron and may accelerate Fe^0 corrosion.[3-7] There are two well-documented routes for Fe^0 corrosion under anaerobic conditions. One route is the oxidation of Fe^0 to Fe^{2+} with the production of H_2:

$$Fe^0+2H^+ \rightarrow Fe^{2+}+H_2 \quad (1)$$

Methanogens consume the H_2 produced from corroding Fe^0, reducing carbon dioxide to methane.[5,8-11] Hydrogenases that are either exported to the outer cell surface or are released during cell lysis can accelerate this reaction (1).[8,10,11] Furthermore, formate dehydrogenases released from cells can catalyze the production of formate from Fe^0, generating another electron donor commonly utilized by H_2-utilizing methanogens:[8,12]

$$Fe^0+H^++CO_2 \rightarrow Fe^{2+}+HCOO^- \quad (2)$$

Some methanogens do not require H_2 or formate intermediary electron carriers to obtain electrons from Fe^0.[9,13] They are capable of electrobiocorrosion, i.e. direct Fe^0-to-microbe electron transfer:[3]

$$4Fe^0+CO_2+8H^+ \xrightarrow{\text{microbe}} 4Fe^{2+}+CH_4+2H_2O \quad (3)$$

Electrobiocorrosion is of interest because it allows electrocorrosive microbes to attack stainless steel alloys of iron that are normally resistant to corrosion by microbes relying on Fe^0 oxidation through H_2 or formate intermediaries.[9,14] Stainless steel contains chromium that forms a 'passivation layer' of chromium oxide on the outer surface of the alloy that prevents abiotic electron transfer for the reduction of protons to H_2.[15] However, the passivation layer does not prevent electrobiocorrosion.[9,13-15]

Microbes capable of electrobiocorrosion include *Geobacter*,[15,16] *Shewanella*,[17,18] *Methanosarcina*[9,13] and *Methanothrix*[9] species. Optimal electrobiocorrosion by *Geobacter*[15,16] and *Shewanella*[17,18] species, as well as *Methanosarcina acetivorans*[13] require outer-surface *c*-type cytochromes previously identified as electrical contacts for electron transfer out of the cell to extracellular electron acceptors. The mechanisms for electron uptake by *Methanosarcina vacuolata* and *Methanothrix soehngenii*, which lack outer-surface *c*-type cytochromes, are unknown.[9] Although *Geobacter*[15,16] and *Shewanella*[17] can grow with Fe^0 as the sole electron donor for electrobiocorrosion, all of the methanogens evaluated to date have required acetate as an additional energy source in order to electrobiocorrode Fe^0.[9,13]

All previously described electrobiocorrosive methanogens are also able to serve as the electron-accepting partner in direct interspecies electron transfer (DIET) with *Geobacter metallireducens* as the electron-donating partner.[19-21] *Methanobacterium subterraneum* strain YSL also grows via DIET with *G. metallireducens*.[22] Therefore, determining whether strain YSL can electrobiocorrode Fe^0 is important for better understanding the diversity of methanogens that can accelerate corrosion with direct electron uptake.

MATERIALS AND METHODS

Strains and growth conditions

Methanobacterium subterraneum strain YSL, whose genome[23] is 97.85% similar to *Methanobacterium subterraneum* A8p, was obtained from the laboratory culture collection. *Methanobacterium formicicum* MF (CCAM 4=DSM 1535) was obtained from the China Collection of Anaerobic Microorganisms (CCAM). Strains YSL and MF were cultured in MA medium[19] in an oxygen-free N_2/CO_2 atmosphere (80/20, v/v, 101 kPa) at 30°C. As previously described, the basic MA medium consisted of the following additions per liter: 0.35 g K_2HPO_4, 0.23 g KH_2PO_4, 0.5 g NH_4Cl, 1 g NaCl, 0.002 g $FeSO_4{\cdot}7H_2O$, 1 mL trace element solution SL-10 (medium DSM320); 10 mmol L^{-1} $NaHCO_3$, and 10 mL Wolin's vitamin solution (medium DSM141). The following solutions were added from sterile anoxic stocks after the basic medium was autoclaved (per liter): 0.3 mmol L^{-1} L-cysteine-HCl, 1 mL 2.7% $CaCl_2{\cdot}2H_2O$, and 1 mL 4.5% $MgSO_4{\cdot}7H_2O$. For continuous cultivation of cultures, sodium formate (60 mmol L^{-1}) or H_2/CO_2 (80/20, 152 kPa) was provided as the electron donor. Prior to growth on Fe^0 granules, both strains YSL and MF were grown with H_2/CO_2 (80/20, 152 kPa) provided as the electron donor for methanogenesis.

Growth on Fe^0

For growth on Fe^0, strains YSL and MF were incubated in 156 mL anaerobic bottles containing 50 mL of MA medium under a N_2/CO_2 (80/20, v/v) atmosphere at 30°C. Ten grams of pure Fe^0 granules (1-2 mm, 99.98% purity metals basis; Alfa Aesar, Shanghai, China) were provided as the sole electron

donor. Prior to use, Fe^0 granules were pre-sterilized with pure ethanol for 5 min and then exposed to UV irradiation for 30 min. The medium was inoculated with 5 mL of strain YSL or MF cells that were grown with H_2/CO_2 as the sole substrate for methanogenesis. Growth on H_2/CO_2 ensured that there was no carryover when cells were inoculated into medium for corrosion studies. In addition, cells were passed three times on medium with Fe^0 granules as the sole source of electrons for methanogenesis before any corrosion data was collected.

To determine whether cells released soluble redox enzymes, cell-free supernatants were prepared from grown cultures as previously described[8] using syringe filters (0.2 μm pore size; Pall Corporation, USA) in an anaerobic chamber. 10 mL of cell filtrate was added to a 30 mL anaerobic tube containing 2 g Fe^0 granules, and flushed with a N_2/CO_2 (80/20, v/v) gas mixture to remove any residual H_2 and CH_4.

Analytical techniques

Methane and hydrogen were analyzed with a gas chromatograph (Agilent Technologies, USA; Model 7820A) equipped with a flame ionization detector (FID) and a thermal conductivity detector (TCD), and the carrier gas was nitrogen. Carbon monoxide was analyzed with a gas chromatograph (Thermo scientific, USA; Model Trace 1300) equipped with a TCD and the carrier gas was argon. The detection limits of hydrogen and carbon monoxide were 1 μmol L^{-1} and 40.86 μmol L^{-1}, respectively.

The concentration of formate was monitored over time using high-performance liquid chromatography (HPLC, Agilent Technologies, USA; Model 1260 Infinity) with a Hi-plexH column equipped with a refractive index detector. The concentration of HCl-extractable Fe(II) was determined with the ferrozine assay as previously described.[24] Protein concentrations were determined by the bicinchoninic acid (BCA) method according to the manufacturer's protocol (Solarbio, China).

Methyl viologen-dependent hydrogenase activity assay

Cultures of strain YSL and MF grown in the presence or absence of Fe^0 granules (10 mL) were pelleted by centrifugation at 5,000 rpm for 10 min at 4°C. Pellets were then suspended in a TE-sucrose buffer (100 mmol L^{-1} Tris-HCl, 1 mmol L^{-1} EDTA, pH 7.5; 6.7% (w/v) sucrose). Extracts were prepared by lysing cells with sonication in an ice-water bath with parameters set at 20 kHz, 1 s/1 s intervals, 2 min and 80 W power. After sonication, extracts were centrifuged at 12,000 rpm for 10 min at 4°C to remove insoluble particles. The crude extracts of strain YSL, strain MF, strain YSL with Fe^0 and strain MF with Fe^0 were quantified with the BCA method and used as sources of hydrogenase.

The hydrogenase assay was performed according to the previously reported method.[25] In a Coy anaerobic chamber, 2 mL reaction mixtures were prepared in 17 mL anaerobic tubes (prefilled with N_2) containing 0.2 mL crude extracts quantified with the BCA method, 0.2 mL 1 mol L^{-1} Tris-HCl (pH 7), 0.2 mL 50 mmol L^{-1} reduced methyl viologen solution, which was freshly prepared by mixing 50 mmol L^{-1} methyl viologen (MV^{2+}, Sigma-Aldrich, USA) 250 mmol L^{-1} sodium dithionite ($Na_2S_2O_4$), and 1.4 mL sterile deionized water. Every 30 min after incubation at 37°C, H_2 in the headspace was monitored by gas chromatography. After 4 hours of incubation, hydrogenase activity was calculated from the amount of H_2 produced from reduced methyl viologen according to the following equation:

Hydrogenase activity (μmol h^{-1} mg $protein^{-1}$) =

$$\frac{\text{Amount of } H_2 \text{ produced}}{\text{Time} \times \text{amount of protein added}}$$

4D-direct data independent acquisition (DIA)-based proteomic analyses

Triplicate cultures (50 mL each) of strain YSL or strain MF cells grown on Fe^0 granules were pelleted by centrifugation at 5,000 rpm for 10 min at 4°C, and then transferred into 2 mL tubes. Total proteins were extracted according to standard procedures. Briefly, the pellets (about 0.2 mL) in each tube were dissolved in 800 μL of extraction buffer (0.7 mol L^{-1} sucrose, 0.1 mol L^{-1} NaCl, 50 mmol L^{-1} EDTA, 13 mmol L^{-1} DTT, 0.5 mol L^{-1} 4 × Tris-HCl pH 6.8, 1.5 mol L^{-1} 4 × Tris-HCl pH 8.8) with the addition of the phosphatase inhibitor cocktail A (50 ×), phenylmethylsulfonyl fluoride (PMSF) at a final concentration of 1 mmol L^{-1}, and steel beads, and then thoroughly ground by a grinder at -35°C, 60 Hz, 120 s for 16 repetitions. After that, 800 μL of Tris-saturated phenol (pH 7.8) was added and samples were mixed for 40 min at 4°C. The supernatant was collected and 5 times the volume of pre-cooled 0.1 mol L^{-1} ammonium acetate-methanol solution was added and samples were precipitated at -40°C overnight. The precipitate was then washed with 5 times the volume of pre-cooled methanol and acetone, respectively. After the washing step, the precipitate was dried and dissolved in 100 μL of SDS lysis buffer (50 mmol L^{-1} Tris pH 8.1, 1% (w/v) SDS, 50×phosphatase inhibitor cocktail A) supplemented with 1 mmol L^{-1} PMSF. Finally, the supernatant was collected by centrifugation and this step was repeated once.

Total protein was quantified with the BCA assay and its integrity was visualized with SDS polyacrylamide gel electrophoresis (SDS-PAGE) prior to trypsin enzymolysis. Prior to trypsin digestion, protein (50 μg) samples were denatured with DTT (final concentration 5 mmol L^{-1}) by incubation at 55°C for 60 min followed by cooling on ice. Iodoacetamide (final concentration 10 mmol L^{-1}) and 6 times the volume of pre-cooled acetone were then added to the solution and proteins were precipitated overnight at -20°C. The precipitate was collected by centrifugation at 8,000 rpm for 10 min at 4°C and dissolved in 100 μL 50 mmol L^{-1} NH_4HCO_3 solution. 1mg mL^{-1} Trypsin-TPCK was added to the solution to digest the proteins with a protein: trypsin ratio of 50: 1 (w/w) at 37°C for 12 h. The enzymatic reaction was stopped by pH adjustment to 3 using phosphoric acid.

Proteomic analyses were conducted on triplicate YSL and MF samples. Digested peptides were desalted on SOLA™ SPE and iRT peptides (Biognosys, ThermoFisher) were added. All proteomic analyses were performed by Shanghai Luming Biological Technology Co., LTD (Shanghai, China). Both shotgun proteomics and data independent acquisition (DIA) experiments used a TimsTOF Pro2 mass spectrometer (Bruker Daltonics) and a nanoElute liquid chromatography system (Bruker Daltonics). Spectronaut Pulsar 17.5 software (Quasar) was used to search all of the raw DIA data against the protein databases of strain MF (GenBank accession no. GCA_000953115.1) and strain YSL (GenBank accession no. GCA_019351055.1). Main parameters of the software were set as follows: Precursor Qvalue cutoff and Protein Qvalue cutoff were set as 0.01, Normalization Strategy was set as Local Normalization, and MS2 was used as the Quantity MS-Level.

The missing value problem with the proteomics data was overcome in accordance with https://datascienceplus.com/proteomics-data-analysis-2-3-data-filtering-and-missing-value-imputation/. A $\log_2$ transformation of the raw data was performed and then the proteins quantified in at least two out of three replicates were retained. After the data was cleaned and filtered, a global median normalization was performed on the filtered proteins. Data imputation on filtered and normalized proteins was then conducted according to previously described methods.[26]

A $\log_2$ (Fold change) ≥ 1 and a P value < 0.05 were used as thresholds to identify differentially expressed proteins (DEPs) by comparing protein expression levels from strain YSL and strain MF cells grown with Fe^0.

The proteomics data in this study have been deposited in the ProteomeXchange Consortium (https://proteomecentral.proteomexchange.org) via the iProX partner repository[27,28] with the dataset identifier PXD050072.

RESULTS AND DISCUSSION

Evaluation of growth on Fe^0 and stainless steel

Strain YSL was grown with either pure Fe^0 or 316L stainless steel as the potential electron donor to evaluate its ability to accept electrons from Fe^0. As expected from previous studies,[16,17] H_2 accumulated over time in uninoculated controls with pure Fe^0 (Figure 1A). Although strain YSL was previously reported to be unable to grow with H_2 as the electron donor,[22] there was no accumulation of H_2 in the presence of cells with a steady production of methane over time. The slope of the line for H_2 generation in the uninoculated control was 3.9-fold higher than the slope of the line for methane production in the strain YSL incubation (Figure 1A), corresponding well with the expected 4:1 stoichiometry of H_2 consumption to methane production. Thus, these results suggest that strain YSL was consuming the H_2 that was being generated from Fe^0.

Analysis of filtrates from cultures growing on Fe^0 indicated that YSL was not releasing factors promoting formation of H_2, or other potential intermedi-

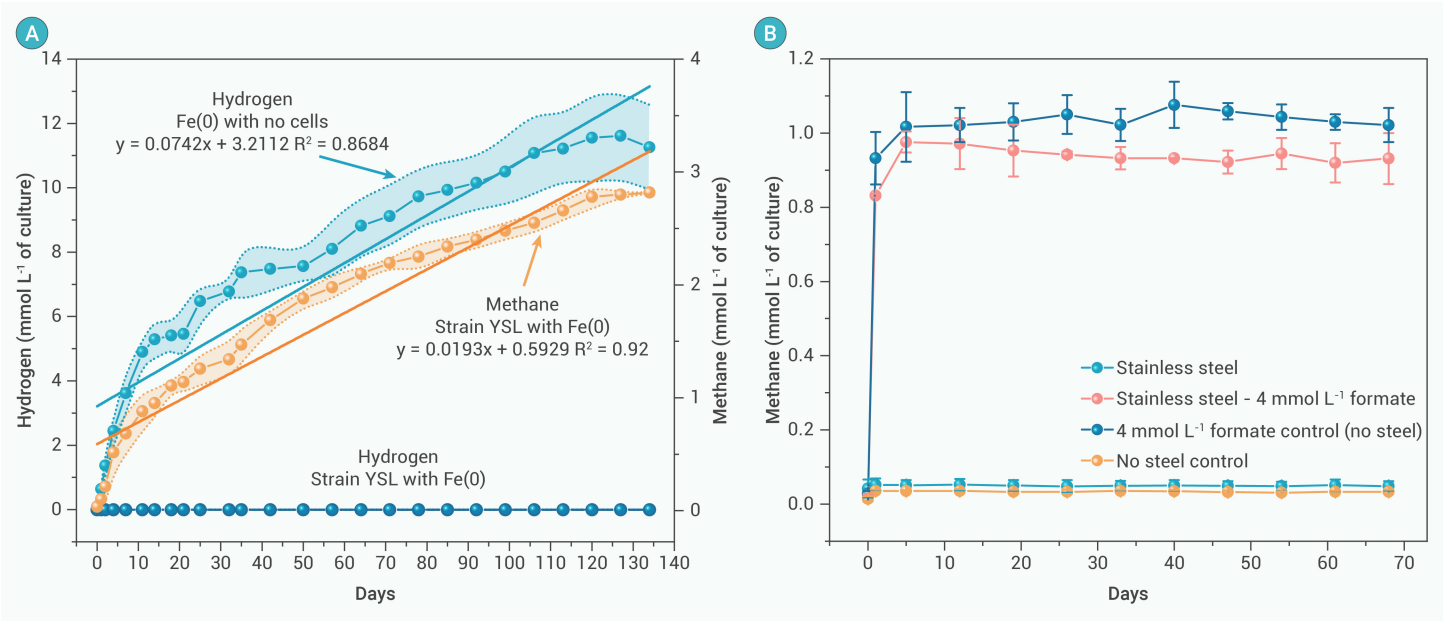

Figure 1. Growth of YSL with Fe(0) granules or stainless steel provided as an electron donor for methanogenesis (A) Methane and H_2 production by YSL cultures grown in the presence of Fe(0) granules. Data are represented as mean values ± standard deviation based on triplicate cultures. Equations represent the linear relationship between hydrogen/methane concentration and incubation time. (B) Methane production by YSL cultures grown in the presence of stainless steel with or without formate (4 mmol L^{-1}). All points represent averages and standard deviations from triplicate cultures.

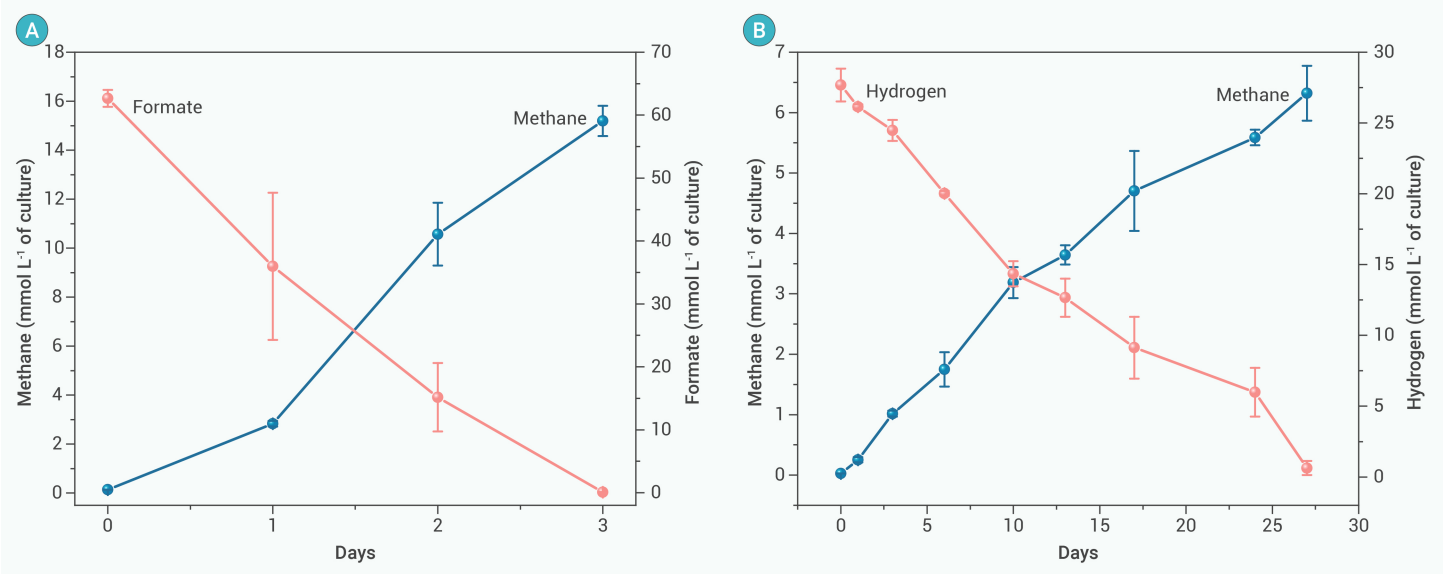

Figure 2. Growth of strain YSL with formate or H_2/CO_2 provided as substrates for methanogenesis (A) Methane and formate concentrations measured in cultures grown with formate (60 mmol L^{-1}) as the sole substrate; (B) Methane and H_2 concentrations measured in cultures grown with H_2/CO_2 as the electron donor. All points represent averages and standard deviations from triplicate cultures.

ary electron carriers such as formate or carbon monoxide (Figure S1).

Strain YSL did not produce methane with stainless steel as the sole electron donor (Figure 1B). Methanogens previously found to produce methane with stainless steel as the electron donor required an electron donor in addition to stainless steel that was converted to methane concurrently with the methane generation from the electrons from stainless steel.[9,13] Therefore, strain YSL was also incubated with both stainless steel and formate, an electron donor known to support growth.[22] The methane produced with stainless steel and formate was not more than with formate alone. In both instances, the 4 mmol L^{-1} formate added yielded slightly less than the 1 mmol L^{-1} of methane expected for conversion of formate to methane. These results demonstrated that strain YSL was unable to obtain electrons from stainless steel.

Strain YSL's apparent consumption of H_2 during growth on Fe^0 and its inability to accept electrons from stainless steel suggest that it requires H_2 as an intermediary electron carrier to obtain electrons from Fe^0. This contrasts with all other microbes that can serve as an electron-accepting partner for DIET that have been evaluated, which are also capable of directly accepting electrons from Fe^0.[9,13,14,16]

Hydrogenotrophic growth

The apparent utilization of H_2 during strain YSL growth on Fe^0 was surprising because it was previously reported to be unable to grow with H_2 as the electron donor.[22] In those studies, cells were grown on an organic-rich medium (MS medium) supplemented with peptone (0.5 g L^{-1}) and tryptone (0.5 g L^{-1}).[22] In contrast, growth on Fe^0 (Figure 1) was conducted in a medium devoid of complex organics to avoid the possibility of unknown organics mediating electron transfer. This medium (MA medium,[19] modified to contain only 1 g L^{-1} NaCl) was optimized for YSL growth, and did not contain any peptone or tryptone. To determine optimal conditions for YSL growth on MA

Table 1. Mutations in hydrogenase related genes within the *Methanobacterium* strain YSL genome that would impact protein structure and function Polymorphisms were identified by comparison to the *M. subterraneum* A8p genome. Only polymorphisms that changed amino acid groups, and that had variant frequencies > 95% and e-values < 0 are included in the table. Further information regarding these genetic variants and other variants in the YSL genome is available in Table S1.

Locus Tag	Gene	Annotation	CDS position	Amino acid change	Amino acid grouping change
KTG15_06555	*ehaA*	Transmembrane protein EhaA	38	Ala→Gly	Hydrophobic to Neutral/nonpolar
KTG15_06505	*ehaK*	Transmembrane protein EhaK	78	Ser→Ala	Polar uncharged to hydrophobic aliphatic
KTG15_06500	*ehaL*	Transmembrane protein EhaL	106	Asp→Lys	Acidic to basic
KTG15_06495	*ehaM*	Cytoplasmic protein EhaM	374	Gln→Pro	Polar uncharged to cyclic/rigid proline
KTG15_06495	*ehaM*	Cytoplasmic protein EhaM	247	Lys→Glu	Basic to acidic
KTG15_06495	*ehaM*	Cytoplasmic protein EhaM	140	Gly→Glu	Neutral/nonpolar to acidic
KTG15_06490	*ehaN*	Ni,Fe-hydrogenase III small subunit	439	Gln→Lys	Polar uncharged to basic
KTG15_06490	*ehaN*	Ni,Fe-hydrogenase III small subunit	187	Pro→Ala	Cyclic/rigid proline to hydrophobic aliphatic
KTG15_06470	*ehaR*	Cytoplasmic protein EhaR	1000	Lys→Glu	Basic to acidic
KTG15_06506	*ehaJ*	Transmembrane protein EhaJ	639	Met→Ile	Thioether side group to branched side group
KTG15_11345	*mvhA1*	F_{420}-non-reducing hydrogenase large subunit	1036	Ala→Thr	Hydrophobic aliphatic to polar uncharged
KTG15_00440	*hypF*	[NiFe] hydrogenase maturation protein	463	Glu→Lys	Acidic to basic
KTG15_00440	*hypF*	[NiFe] hydrogenase maturation protein	235	Asp→Asn	Acidic to polar uncharged
KTG15_00440	*hypF*	[NiFe] hydrogenase maturation protein	349	Ile→Phe	Hydrophobic aliphatic to hydrophobic aromatic
KTG15_00440	*hypF*	[NiFe] hydrogenase maturation protein	283	His→Asn	Basic to polar uncharged
KTG15_00440	*hypF*	[NiFe] hydrogenase maturation protein	341	Asp→Ala	Acidic to hydrophobic aliphatic
KTG15_00440	*hypF*	[NiFe] hydrogenase maturation protein	241	Lys→Gln	Basic to polar uncharged
KTG15_00440	*hypF*	[NiFe] hydrogenase maturation protein	1876	Glu→Lys	Acidic to basic
KTG15_00440	*hypF*	[NiFe] hydrogenase maturation protein	1490	Phe→Ser	Hydrophobic aromatic to polar uncharged
KTG15_00440	*hypF*	[NiFe] hydrogenase maturation protein	238	Asp→Asn	Acidic to polar uncharged
KTG15_00440	*hypF*	[NiFe] hydrogenase maturation protein	91	Asn→Asp	Polar uncharged to acidic
KTG15_00440	*hypF*	[NiFe] hydrogenase maturation protein	211	Ser→Arg	Polar uncharged to basic
KTG15_00440	*hypF*	[NiFe] hydrogenase maturation protein	199	Ser→Ala	Polar uncharged to hydrophobic aliphatic
KTG15_00440	*hypF*	[NiFe] hydrogenase maturation protein	161	Ile→Ser	Hydrophobic aliphatic to polar uncharged
KTG15_00440	*hypF*	[NiFe] hydrogenase maturation protein	169	Asp→Tyr	Acidic to hydrophobic aromatic

medium, different NaCl concentrations (0.5 to 3 g L^{-1}), temperature (25ºC to 37ºC), and pH values (pH 6.5 to pH 7.5) were tested. YSL grew best when it was incubated at 30ºC in medium adjusted to pH 7 with 1 g L^{-1} NaCl. Cells grew (Figure 2A) faster on formate in the MA medium (doubling time 17.1 hours) than previously described MS medium (doubling time 48.5 hours).

Strain YSL also slowly grew (doubling time 131.1 h) in MA medium with H_2 as the electron donor (Figure 2B). This is more than 50-fold slower than the 2.5 h doubling time for the A8p strain of *M. subterraneum* sp.[29] and the 2.2 h doubling time for the closely related *M. formicicum* MF.[30] Hydrogenase activity was detected in lysed strain YSL cells, but it was 2-fold lower than in lysates of *M. formicicum* MF (Figure S2).

Genome analysis

The strain YSL genome was analyzed to further evaluate its potential for growth on H_2. This included a comparison with the genome of *M. subterraneum* strain A8p, which is 97.9% identical to the strain YSL genome, to identify nucleotide substitutions that could impact the function of hydrogenases.

Multiple genes encoding hydrogenases are present in the strain YSL genome. One hydrogenase gene cluster encodes EhaA-T, which is the primary membrane-bound [NiFe] hydrogenase for energy conservation from H_2 oxidation by *Methanobacteriales* species.[31-34] Deletion of Eha impairs the growth of many hydrogenotrophic methanogens on H_2/CO_2.[31] It is thought to be primarily involved in the reduction of CO_2 to formylmethanofuran through reduction of ferrodoxin. Compared to the *M. subterraneum* strain A8p genome, the YSL genome contained nucleotide polymorphisms that could impact protein function in genes for seven different Eha subunits (*ehaA, ehaJ, ehaK, ehaL, ehaM, ehaN*, and *ehaR*), four of which are transmembrane components (Tables 1 & S1, Figure S3A). None of these mutations were synonymous and all of them would lead to major amino acid substitutions (e.g. hydrophobic to neutral, polar to nonpolar, acidic to basic, nonpolar to acidic, polar to basic) that are predicted to disrupt protein folding and enzymatic function.

Protein prediction software (AlpaFold Server (https://alphafoldserver.com/) and JPred (https://www.compbio.dundee.ac.uk/jpred4)) indicated that these mutations would alter both the secondary and tertiary structures of the Eha subunits, thereby impairing their ability to assemble into the larger multisubunit hydrogenase complex (Figure S3). In addition, two missense mutations were found in the critical EhaN subunit, which encodes the NiFe hydrogenase small subunit. These mutations result in the replacement of a polar uncharged amino acid with a basic one, as well as substitution of a cyclic, structurally rigid proline with a smaller and more flexible alanine. Prediction software indicates that EhaN in strain YSL contains four ß-strands and five helices, compared to five beta strands and six α-helices in strain A8p, and that the tertiary structure of EhaN in strain A8p is more globular. These structural differences in EhaN, together with substantial mutations in six additional Eha subunits, strongly suggest that the Eha hydrogenase complex in

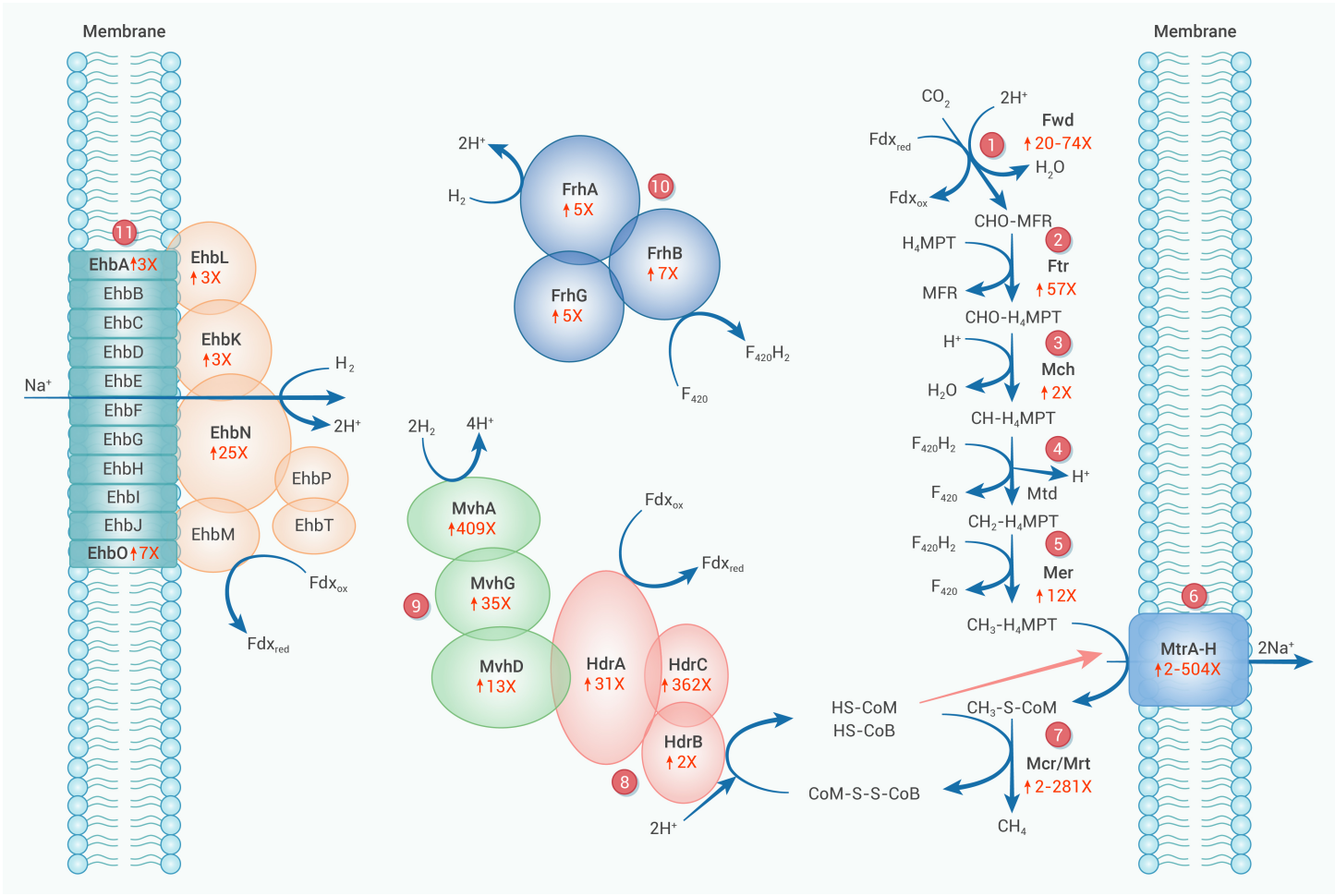

Figure 3. Proposed pathway for H_2 oxidation during growth on Fe(0) by strain YSL Up arrows represent fold-up regulation of proteins expressed by strain YSL compared to strain MF during growth with Fe(0) as the sole electron donor. (1) Fwd: formylmethanofuran dehydrogenase; (2) Ftr: formylmethanofuran-tetrahydromethanopterin formyltransferase; (3) Mch: methenyltetrahydromethanopterin cyclohydrolase; (4) Mtd: methylenetetrahydromethanopterin dehydrogenase; (5) Mer: 5,10-methylenetetrahydromethanopterin reductase; (6) Mtr: tetrahydromethanopterin S-methyltransferase; (7) Mcr/Mrt: methyl-coenzyme M reductase Ⅰ/methyl-coenzyme M reductase Ⅱ; (8) Hdr: CoB-CoM heterodisulfide reductase; (9) Mvh: F_{420}-non-reducing hydrogenase; (10) Frh: coenzyme F_{420} hydrogenase. (11) Ehb: energy-converting hydrogenase B. Source data are provided in Table S2.

strain YSL is functionally impaired. However, experimental studies will be required to confirm this.

The strain YSL genome also has genes for EhbA-Q, a membrane-bound [NiFe] hydrogenase thought to be primarily involved in autotrophic carbon dioxide fixation,[31,32,35] and FrhABG, a cytoplasmic coenzyme F_{420}-reducing [NiFe]-hydrogenase.[34] In comparison with the *M. subterraneum* strain A8p genome, there were no apparent mutations in the genes for these hydrogenases that would impair function.

Methanobacterium species utilize an electron bifurcating heterodisulfide reductase (HdrABC)-[NiFe]-hydrogenase (MvhAGD) complex to intracellularly oxidize H_2 and reduce ferredoxin and the heterodisulfide of coenzymes M and B.[36,37] The genome has two copies of both MvhAGD and HdrABC complexes. Mutations were detected in one of the two MvhA subunits (Table 1). However, no polymorphisms were found in the other copy of MvhA. Thus, MvhAGD-HdrABC function is unlikely to be impaired.

Neither the YSL nor the A8p strain of *M. subterraneum* appears to encode Hmd. This [Fe] hydrogenase is a component of the methylene tetrahydromethanopterin dehydrogenase complex ([Fe]-hydrogenase), which is present in many other cytochrome-deficient hydrogenotrophic methanogens, including other *Methanobacterium* species.[34,38]

A functional HypABCDE [NiFe] hydrogenase maturation complex is required for proper [NiFe] hydrogenase function in methanogens.[39] No mutations were found in the HypA-E genes. However, fourteen base substitutions are present in the gene for HypF (Tables 1 & S1). In bacteria,[40-43] and the hyperthermophilic archaeon, *Thermococcus kodakarensis*,[44] HypF is involved in synthesizing cyanide ligands located in the active sites of [NiFe] hydrogenases. Analysis of the secondary and tertiary structure of HypF in YSL indicates that this protein is structurally different from that found in A8p; HypF in strain YSL is predicted to have 27 beta strands and 22 alpha helices compared to 25 beta strands and 23 alpha helices in strain A8p (Figure S4). The significance of HypF in hydrogenotrophic methanogens is not known.[39,45] However, the finding that other NiFe hydrogenases were functional in YSL indicates that HypF is either not required for assembly of the NiFe active site in *Methanobacterium* species or its modified structure does not impact its functionality.

Thus, the most likely possibility for the very poor growth of strain YSL on H_2 is that the function of the Eha hydrogenase complex is disrupted. The strain YSL genome has genes coding for a cytoplasmic formate dehydrogenase complex (FdhAB) that can couple the oxidation of formate with reduction of F_{420} and it can also interact with MvhD-HdrABC for the flavin-based electron bifurcating reduction of ferredoxin and coenzymes M and B.[46,47] The presence of these genes and the finding that none of these genes have mutations explains how strain YSL can grow on formate.

Proteomic analysis of electron uptake by strain YSL from Fe^0

To further explore potential mechanisms for electron uptake by strain YSL from Fe^0, 4D-direct DIA (data-independent acquisition) based proteomic comparisons were made between Fe^0-grown cells of strain YSL and the closely related *M. formicicum* strain MF, which can efficiently grow on H_2/CO_2 and Fe^0 granules at rates that are ~2.2 times faster than strain YSL (Table S2). Principal component analysis (PCA) showed that there were distinct differences in the proteomic profiles of the two strains (Figure S5).

479 proteins were more highly expressed in strain YSL (P value < 0.05) (Table S2A) and 223 different proteins were more highly expressed in strain MF (P value < 0.05) (Table S2B).

A few of the Eha subunits were somewhat more highly expressed in strain YSL (EhaQ, EhaP, and EhaC; 2.4, 4.3, and 5.4 times more highly expressed, respectively), but none of these subunits are involved in H_2 oxidation (Table S2A). Multiple Ehb subunits (EhbA, EhbK, EhbL, EhbN, EhbM, and EhbO) were more highly expressed by strain YSL than strain MF (Figure 3 & Table S2A). Notably, EhbN, the catalytic subunit of the Ehb complex, was 25.2 times (P value < 0.0003) more abundant in strain YSL.

Cytoplasmic hydrogenase subunits were much more highly expressed in strain YSL (Figure 3 & Table S2A). FrhABG was 4.8 to 7.4 times (P values < 0.02) more highly expressed, and the functional MvhABGD subunits were 408.8, 98.9, 12.8, and 35.2 times (P values < 0.0002) more highly expressed in strain YSL. HdrABC subunits were 31.3, 2.3, and 362.1 times (P values < 0.01) more highly expressed. In contrast, there was no differential expression of formate dehydrogenase proteins between the two strains. These results suggest that the mutations in the Eha complex genes negatively affect Eha function and that, in order to compensate, cytoplasmic hydrogenases and, to some extent, Ehb hydrogenase are more highly expressed, enabling slow growth on H_2.

CONCLUSION

The results demonstrate that in contrast to an earlier report, strain YSL can grow, albeit slowly, with H_2 as the electron donor. Although strain YSL's rate of H_2 consumption is much lower than that of the hydrogenotrophic methanogens that have been investigated most extensively in laboratory culture, it is more than sufficient to match the slow release of H_2 that is associated with Fe^0 corrosion. This finding emphasizes the potential environmental importance of microbial reactions that are slow by traditional laboratory standards.

Unlike the closely related *M. formicicum*, which did not grow via DIET,[48] strain YSL appears to directly receive electrons during DIET-based growth with *G. metallireducens*.[22] Strain YSL's ability to use H_2 and formate is not considered to be a factor in its DIET-based co-culture with *G. metallireducens* because *G. metallireducens* does not generate H_2 or formate during the metabolism of ethanol, the substrate used for these DIET studies.[48-51]

However, strain YSL's ability to slowly consume H_2 appeared to be an important factor in its growth with Fe^0 as the electron donor. No H_2 accumulated over time and the rate of methane production matched the amount of methane production possible from the slow abiotic production of H_2 from Fe^0 in the uninoculated controls. These results and the finding that strain YSL did not produce methane with stainless steel as the electron donor suggest that strain YSL is not capable of electrobiocorrosion. This finding is surprising, as all other microbes tested that act as electron-accepting partners for DIET can also directly utilize electrons from Fe^0 without H_2 as an intermediary carrier.[9,13,15,16]

The full range of mechanisms for electrotrophy during DIET and electrobiocorrosion are unknown. Although outer-surface *c*-type cytochromes have often been implicated as electrical contacts for both DIET and electrobiocorrosion,[3,15-17,52] a number of electrotrophs involved in these processes lack outer-surface cytochrome electrical connects.[9,21,48,53-56] Their mechanisms for electron uptake are unknown.

Although strain YSL was not capable of electrobiocorrosion, it employed a unique mechanism for H_2-based corrosion. Unlike other hydrogenotrophic methanogens such as strain MF, strain YSL did not highly express membrane-bound hydrogenase complexes during growth on Fe^0 granules. Instead, it relied primarily on cytoplasmic hydrogenases to support hydrogenotrophic growth. While the genomes of strains MF and YSL are similar, and both have comparable growth rates on formate, their differing hydrogenase profiles significantly influenced H_2-corrosion rates. As a result, strain YSL grew more than two-fold slower than strain MF when Fe^0 granules were provided as the electron donor.

The results presented here demonstrate that strain YSL will not be a useful model for electrobiocorrosion. However, further comparisons of strain YSL and closely related *Methanobacterium* strains that do not grow via DIET could provide insights into DIET electron uptake mechanisms that do not rely on cytochromes.

REFERENCES

1. Knisz J., Eckert R., Gieg L.M., et al. (2023). Microbiologically influenced corrosion-more than just microorganisms. *FEMS Microbiol. Rev.* **47**:fuad041. DOI:10.1093/femsre/fuad041
2. Little B.J., Hinks J. and Blackwood D.J. (2020). Microbially influenced corrosion: Towards an interdisciplinary perspective on mechanisms. *Int. Biodeterior. Biodegr.* **154**:105062. DOI:10.1016/j.ibiod.2020.105062
3. Xu D.K., Gu T.Y. and Lovley D.R. (2023). Microbially mediated metal corrosion. *Nat. Rev. Microbiol.* **21**:705–718. DOI:10.1038/s41579-023-00920-3
4. Daniels L., Belay N., Rajagopal B.S., et al. (1987). Bacterial methanogenesis and growth from CO_2 with elemental iron as the sole source of electrons. *Science* **237**:509–511. DOI:10.1126/science.237.4814.509
5. Lahme S., Mand J., Longwell J., et al. (2021). Severe corrosion of carbon steel in oil field produced water can be linked to methanogenic archaea containing a special type of [NiFe] hydrogenase. *Appl. Environ. Microbiol.* **87**:e01819–01820. DOI:10.1128/aem.01819-20
6. Tamisier M., Schmidt M., Vogt C., et al. (2022). Iron corrosion by methanogenic archaea characterized by stable isotope effects and crust mineralogy. *Environ. Microbiol.* **24**:583–595. DOI:10.1111/1462-2920.15658
7. Usher K.M., Kaksonen A.H. and MacLeod I.D. (2014). Marine rust tubercles harbour iron corroding archaea and sulphate reducing bacteria. *Corros. Sci.* **83**:189–197. DOI:10.1016/j.corsci.2014.02.014
8. Deutzmann J.S., Sahin M. and Spormann A.M. (2015). Extracellular enzymes facilitate electron uptake in biocorrosion and bioelectrosynthesis. *mBio* **6**:e00496–00415. DOI:10.1128/mBio.00496-15
9. Holmes D.E., Woodard T.L., Smith J.A., et al. (2024). Electrobiocorrosion by microbes without outer-surface cytochromes. *mLife* **3**:110–118. DOI:10.1002/mlf2.12111
10. Kawaichi S., Kotoky R., Fiutowski J., et al. (2024). Adaptation of a methanogen to Fe^0 corrosion via direct contact. *Npj Biofilms and Microbi.* **10**:100. DOI:10.1038/s41522-024-00574-w
11. Tsurumaru H., Ito N., Mori K., et al. (2018). An extracellular [NiFe] hydrogenase mediating iron corrosion is encoded in a genetically unstable genomic island in *Methanococcus maripaludis*. *Sci. Rep.* **8**:15149. DOI:10.1038/s41598-018-33541-5
12. Lienemann M., Deutzmann J.S., Milton R.D., et al. (2018). Mediator-free enzymatic electrosynthesis of formate by the *Methanococcus maripaludis* heterodisulfide reductase supercomplex. *Bioresource Technol.* **254**:278–283. DOI:10.1016/j.biortech.2018.01.036
13. Holmes D.E., Tang H., Woodard T.L., et al. (2022). Cytochrome - mediated direct electron uptake from metallic iron by *Methanosarcina acetivorans*. *mLife* **1**:443–447. DOI:10.1002/mlf2.12044
14. Liang D.D., Liu X.Y., Woodard T.L., et al. (2021). Extracellular electron exchange capabilities of *Desulfovibrio ferrophilus* and *Desulfopila corrodens*. *Environ. Sci. Technol.* **55**:16195–16203. DOI:10.1021/acs.est.1c04071
15. Tang H.-Y., Yang C., Ueki T., et al. (2021). Stainless steel corrosion via direct iron-to-microbe electron transfer by *Geobacter* species. *The ISME J.* **15**:3084–3093. DOI:10.1038/s41396-021-00990-2
16. Tang H.-Y., Holmes D.E., Ueki T., et al. (2019). Iron corrosion via direct metal-microbe electron transfer. *mBio* **10**:e00303–00319. DOI:10.1128/mBio.00303-19
17. Hernandez-Santana A., Suflita J.M. and Nanny M.A. (2022). *Shewanella oneidensis* MR-1 accelerates the corrosion of carbon steel using multiple electron transfer mechanisms. *Int. Biodeterior. Biodegr.* **173**:105439. DOI:10.1016/j.ibiod.2022.105439
18. Zhou E.Z., Li F., Zhang D.W., et al. (2022). Direct microbial electron uptake as a mechanism for stainless steel corrosion in aerobic environments. *Water Res.* **219**:118553. DOI:10.1016/j.watres.2022.118553
19. Holmes D.E., Zhou J.J., Ueki T., et al. (2021). Mechanisms for electron uptake by *Methanosarcina acetivorans* during direct interspecies electron transfer. *mBio* **12**:e0234421. DOI:10.1128/mBio.02344-21
20. Yee M.O. and Rotaru A.-E. (2020). Extracellular electron uptake in Methanosarcinales is independent of multiheme *c*-type cytochromes. *Sci. Rep.* **10**:747485. DOI:10.1101/747485
21. Zhou J.J., Holmes D.E., Tang, H.-Y., et al. (2021). Correlation of key physiological properties of *Methanosarcina* isolates with environment of origin. *Appl. Environ. Microbiol.* **87**:e00731–00721. DOI:10.1128/aem.00731-21
22. Zheng S.L., Liu F.H., Wang B.C., et al. (2020). *Methanobacterium* capable of direct interspecies electron transfer. *Environ. Sci. Technol.* **54**:15347–15354. DOI:10.1021/acs.est.0c05525
23. Zheng S.L. and Liu F.H. (2021). Complete genome sequence of *Methanobacterium electrotrophus* strain YSL, isolated from coastal riverine sediments. *Microbiol. Resour. Ann* **10**:e0075221. DOI:10.1128/mra.00752-21
24. Lovley D.R. and Phillips E.J.P. (1987). Rapid assay for microbially reducible ferric iron in aquatic sediments. *Appl. Environ. Microbiol.* **53**:1536–1540. DOI:10.1128/aem.53.7.1536-1540.1987
25. Kosem N. (2023). H_2 production from methyl viologen-dependent hydrogenase activity monitored by gas chromatography. *Bio-protocol* **13**:e4895. DOI:10.21769/BioProtoc.4895

26. Lazar C., Gatto L., Ferro M., et al. (2016). Accounting for the multiple natures of missing values in label-free quantitative proteomics data sets to compare imputation strategies. *J. Proteome Res.* **15**:1116–1125. DOI:10.1021/acs.jproteome.5b00981
27. Chen T., Ma J., Liu Y., et al. (2022). iProX in 2021: Connecting proteomics data sharing with big data. *Nucleic Acids Res.* **50**:D1522–D1527. DOI:10.1093/nar/gkab1081
28. Ma J., Chen T., Wu S.F., et al. (2019). iProX: An integrated proteome resource. *Nucleic Acids Res.* **47**:D1211–D1217. DOI:10.1093/nar/gky869
29. Kotelnikova S., Macario A.J. and Pedersen K. (1998). *Methanobacterium subterraneum* sp. *nov., a new alkaliphilic, eurythermic and halotolerant methanogen isolated from deep granitic groundwater. Int. J. Syst. Evol. Microbiol.* **48**:357–367. DOI:10.1099/00207713-48-2-357
30. Wu W.M., Hickey R.F., Jain M.K., et al. (1993). Energetics and regulations of formate and hydrogen metabolism by *Methanobacterium formicicum. Arch. Microbiol.* **159**:57–65. DOI:10.1007/bf00244265
31. Lie T.J., Costa K.C., Lupa B., et al. (2012). Essential anaplerotic role for the energy-converting hydrogenase Eha in hydrogenotrophic methanogenesis. *Proc. Natl. Acad. Sci. USA* **109**:15473–15478. DOI:10.1073/pnas.1208779109
32. Porat I., Kim W., Hendrickson E.L., et al. (2006). Disruption of the operon encoding Ehb hydrogenase limits anabolic CO_2 assimilation in the archaeon *Methanococcus maripaludis. J. Bacteriol.* **188**:1373–1380. DOI:10.1128/jb.188.4.1373-1380.2006
33. Tersteegen A. and Hedderich R. (1999). *Methanobacterium thermoautotrophicum* encodes two multisubunit membrane-bound [NiFe] hydrogenases -: Transcription of the operons and sequence analysis of the deduced proteins. *Eur. J. Biochem.* **264**:930–943. DOI:10.1046/j.1432-1327.1999.00692.x
34. Thauer R.K., Kaster A.K., Goenrich M., et al. (2010). Hydrogenases from methanogenic archaea, nickel, a novel cofactor, and H_2 storage. Kornberg R.D., Raetz C.R.H., Rothman J.E., et al. (eds). Annual Review of Biochemistry (Annual Reviews), pp:507-536. DOI:10.1146/annurev.biochem.030508.152103
35. Major T.A., Liu Y.C. and Whitman W.B. (2010). Characterization of energy-conserving hydrogenase B in *Methanococcus maripaludis. J. Bacteriol.* **192**:4022–4030. DOI:10.1128/jb.01446-09
36. Appel L., Willistein M., Dahl C., et al. (2021). Functional diversity of prokaryotic HdrA(BC) modules: Role in flavin-based electron bifurcation processes and beyond. *BBA-Bioenergetics* **1862**:148379. DOI:10.1016/j.bbabio.2021.148379
37. Wagner T., Koch J., Ermler U., et al. (2017). Methanogenic heterodisulfide reductase (HdrABC-MvhAGD) uses two noncubane [4Fe-4S] clusters for reduction. *Science* **357**:699–702. DOI:10.1126/science.aan0425
38. Watanabe T., Wagner T., Huang G.F., et al. (2019). The bacterial [Fe]-hydrogenase paralog HmdII uses tetrahydrofolate derivatives as substrates. *Angew. Chem. Int. Edit.* **58**:3506–3510. DOI:10.1002/anie.201813465
39. Guss A.M., Kulkarni G. and Metcalf W.W. (2009). Differences in hydrogenase gene expression between *Methanosarcina acetivorans* and *Methanosarcina barkeri. J. Bacteriol.* **191**:2826–2833. DOI:10.1128/jb.00563-08
40. Blokesch M., Paschos A., Theodoratou E., et al. (2002). Metal insertion into NiFe-hydrogenases. *Biochem. Soc. Trans.* **30**:674–680. DOI:10.1042/bst0300674
41. Buhrke T., Bleijlevens B., Albracht S.P.J., et al. (2001). Involvement of hyp gene products in maturation of the H_2-sensing [NiFe] hydrogenase of *Ralstonia eutropha. J. Bacteriol.* **183**:7087–7093. DOI:10.1128/jb.183.24.7087-7093.2001
42. Lacasse M.J. and Zamble D.B. (2016). [NiFe]-hydrogenase maturation. *Biochemistry-US* **55**:1689–1701. DOI:10.1021/acs.biochem.5b01328
43. Caserta G., Hartmann S., Van Stappen C., et al. (2023). Stepwise assembly of the active site of [NiFe]-hydrogenase. *Nat. Chem. Biol.* **19**:498. DOI:10.1038/s41589-022-01226-w
44. Miki K., Atomi H. and Watanabe S. (2020). Structural insight into [NiFe] hydrogenase maturation by transient complexes between Hyp proteins. *Acc. Chem. Res.* **53**:875–886. DOI:10.1021/acs.accounts.0c00022
45. Sawers R.G., Hardelt M., Haase A., et al. (2025). Biosynthesis and assembly of hydrogenase [NiFe]-cofactor: recent advances and perspectives. *Metallomics* **17**:mfaf015. DOI:10.1093/mtomcs/mfaf015
46. Abdul Halim M.F., Fonseca D.R., Niehaus T.D., et al. (2024). Functionally redundant formate dehydrogenases enable formate-dependent growth in *Methanococcus maripaludis. J. Biol. chem.* **300**:105550. DOI:10.1016/j.jbc.2023.105550
47. Costa K.C., Wong P.M., Wang T.S., et al. (2010). Protein complexing in a methanogen suggests electron bifurcation and electron delivery from formate to heterodisulfide reductase. *Proc. Natl. Acad. Sci. USA* **107**:11050–11055. DOI:10.1073/pnas.1003653107
48. Rotaru A.-E., Shrestha P.M., Liu F.H., et al. (2014). A new model for electron flow during anaerobic digestion: Direct interspecies electron transfer to *Methanosaeta* for the reduction of carbon dioxide to methane. *Energy Environ. Sci.* **7**:408–415. DOI:10.1039/c3ee42189a
49. Rotaru A.E., Shrestha P.M., Liu F.H., et al. (2012). Interspecies electron transfer via hydrogen and formate rather than direct electrical connections in cocultures of *Pelobacter carbinolicus* and *Geobacter sulfurreducens Appl. Environ. Microbiol.* **78**:7645–7651. DOI:10.1128/aem.01946-12
50. Shrestha P.M., Rotaru A.-E., Summers Z.M., et al. (2013). Transcriptomic and genetic analysis of direct interspecies electron transfer. *Appl. Environ. Microbiol.* **79**:2397–2404. DOI:10.1128/aem.03837-12
51. Summers Z.M., Fogarty H.E., Leang C., et al. (2010). Direct exchange of electrons within aggregates of an evolved syntrophic coculture of anaerobic bacteria. *Science* **330**:1413–1415. DOI:10.1126/science.1196526
52. Wang D., Zhou E.Z., Xu D.K., et al. (2023). Burning question: Are there sustainable strategies to prevent microbial metal corrosion. *Microb. Biotechnol.* **16**:2026–2035. DOI:10.1111/1751-7915.14347
53. Holmes D.E., Zhou J.J., Smith J.A., et al. (2022). Different outer membrane *c*-type cytochromes are involved in direct interspecies electron transfer to *Geobacter* or *Methanosarcina* species. *mLife* **1**:272–286. DOI:10.1002/mlf2.12037
54. Holmes D.E., Rotaru A.-E., Ueki T., et al. (2018). Electron and proton flux for carbon dioxide reduction in *Methanosarcina barkeri* during direct interspecies electron transfer. *Front. Microbiol.* **9**:3109. DOI:10.3389/fmicb.2018.03109
55. Rotaru A.-E., Shrestha P.M., Liu F.H., et al. (2014). Direct interspecies electron transfer between *Geobacter metallireducens* and *Methanosarcina barkeri. Appl. Environ. Microbiol.* **80**:4599–4605. DOI:10.1128/aem.00895-14
56. Zhou J.J., Smith J.A., Li M., et al. (2023). Methane production by *Methanothrix thermoacetophila* via direct interspecies electron transfer with *Geobacter metallireducens. mBio* **14**:e00360–00323. DOI:10.1128/mbio.00360-23

FUNDING AND ACKNOWLEDGMENTS

This work was supported by the National Natural Science Foundation of China (grant no. 42273082, U20A20109 and 92251301), the Taishan Scholar Program of Shandong Province (tsqn202306293), the Guangdong Foundation for Program of Science and Technology Research (grant nos. 2020B1111530002 and 2023B1212060044), the GDAS' Project of Science and Technology Development (grant nos. 2019GDASYL-0102003) and the Pearl River Talent Recruitment Program (2019QN01L735) of Guangdong Province, the Program of Dongying (DYYG2024-09). We sincerely thank Prof. Lei Cheng at the Biogas Institute of Ministry of Agriculture and Rural Affairs for kindly providing the methanogen – *Methanobacterium formicicum* MF; Prof. Dake Xu and Dr. Enze Zhou at Northeastern University for support with carbon monoxide analysis. The funders had no role in study design, data collection and analysis, decision to publish, or preparation of the manuscript.

AUTHOR CONTRIBUTIONS

F.L., D.L. and D.H. conceived and designed the study. S.Z. and D.H. performed the experiments and the bioinformatics analysis. X.L conducted GC and HPLC analyses. S.Z. and D.H. drafted the manuscript. D.L. and F.L. critically revised the manuscript. All authors contributed to the manuscript and approved the final version.

DECLARATION OF INTERESTS

The authors declare no competing interests.

DATA AND CODE AVAILABILITY

The proteomics data in this study have been deposited to the ProteomeXchange Consortium (https://proteomecentral.proteomexchange.org) under the ProteomeXchange ID PXD050072.

SUPPLEMENTAL INFORMATION

It can be found online at https://doi.org/10.59717/j.xinn-geo.2025.100166

LEAD CONTACT WEBSITE

Shiling Zheng: https://www.researchgate.net/profile/Shiling-Zheng
Fanghua Liu: https://www.researchgate.net/profile/Fanghua_Liu
https://www.soil.gd.cn/yjsjy/dsjs/t45570.html